Clays and Clay Minerals, Vol. 40, No. 4, 446–456, 1992.

MORPHOLOGY, TEXTURE, AND MICROSTRUCTURE OF HALLOYSITIC SOIL CLAYS AS RELATED TO WEATHERING AND EXCHANGEABLE CATION

B. DELVAUX,[1] D. TESSIER,[2] A. J. HERBILLON,[3] G. BURTIN,[3]
ANNE-MARIE JAUNET,[2] AND L. VIELVOYE[4]

[1] Unité des Sciences du Sol, U.C.L., Place Croix du Sud, 2, bte 10, 1348 Louvain-la-Neuve, Belgium

[2] INRA, Station de Science du Sol, Route de Saint-Cyr, 78026 Versailles Cedex, France

[3] Centre de Pédologie Biologique, UP6831 du CNRS, associée à l'Université de Nancy I, BP 5, 54501 Vandoeuvre-les-Nancy Cedex 1, France

[4] Section de Physico-chimie Minérale, MRAC, Place Croix du Sud, 1, 1348 Louvain-la-Neuve, Belgium

Abstract—This paper aims at characterizing the morphology, texture, and microstructure of three hydrated kaolin rich clays ($f < 0.2$ μm) from volcanic soils. These clays represent a weathering sequence in which CEC, halloysite content with respect to kaolinite, as well as smectite content in the halloysite-smectite mixed-layer clays decrease with increased weathering. The clay samples were made homoionic (K^+ or Mg^{2+}) and hydrated under a low suction pressure (3.2 kPa). After replacing water by a resin, ultrathin sections were cut and examined by TEM. Particle shape varies with increased weathering, as follows: spheroids → tubes → platelets. Higher aggregation and dispersion are observed by TEM after Mg^{2+} and K^+ saturation, respectively, at two levels of the clay-water system organization: intraparticle and interparticle. The microstructure variations induced by the nature of the exchangeable cation become less pronounced with decreasing layer charge of the 2:1 layers. They are thus related here to the presence of smectite layers localized in the halloysite habitus, mostly at the particle periphery. These results show that small amounts of smectite largely affect the organization of clays rich in kaolins at a high water content, and that K^+ behaves here as a dispersing ion.

Key Words—Exchangeable cation, Halloysite, Interstratification, Microstructure, Smectite, TEM.

INTRODUCTION

The texture and microstructure of strongly hydrated clay minerals vary mostly according to their CEC and the nature of the exchangeable cation. Na^+ and K^+ smectites at low suctions are much more hydrated, and thus dispersed, than the same Ca^{2+} and Mg^{2+} saturated clays. These hydration properties distinguish smectites from kaolinites and illites *sensu stricto* (Tessier, 1984 and 1987). As far as homoionic 2:1 swelling clays are concerned, water content and dispersion at low suctions increase with decreasing layer charge, i.e., from vermiculite to low charge smectite (Touret *et al.*, 1990).

Morphological features and charge properties of halloysite are documented in several studies recently reviewed by Bailey (1990), but the microstructure of halloysite at low water suction potential has not yet been fully investigated. Hydrated halloysites are widespread in the clay fraction of soils derived from pyroclastic materials. Under humid tropical conditions, halloysite-rich soils often represent a specific weathering stage antecedent to older soils richer in anhydrous 1:1 clay minerals of kaolinite type. The mineralogical sequence halloysite → kaolinite generally involves a decrease in the clay's CEC (Quantin, 1990). This sequence is observed in volcanic ash soils from Western Cameroon, where the high charge of halloysitic soil clays has been related to the presence of smectite within halloysite-smectite (H-Sm) mixed-layer clays (Delvaux *et al.*, 1990b).

The purpose of this paper is to characterize by TEM the shape, texture, and microstructure of soil clays (<0.2 μm) representing that mineralogical sequence in which H-Sm mixed-layer clays progressively transform into kaolinite as weathering proceeds. For this study, the fine clays were previously made homoionic with respectively K^+ and Mg^{2+}, and then strongly hydrated.

MATERIALS AND METHODS

Clay samples

The clay samples were extracted from the major B horizons of three basaltic ash-derived soils from Western Cameroon: SN5 (Tropept), SN2 (Udalf), and MK1 (Udult). The pedons derive from similar parent material and have reached different stages of weathering (Delvaux *et al.*, 1989). The clays differ in their relative halloysite content with respect to kaolinite [H/(H + K)], CEC and K^+ affinity. With increasing soil weathering, a decrease is observed in relative halloysite content, CEC, K^+ affinity, and also content and layer charge of the smectite units involved in the halloysite/smectite

(H/Sm) mixed-layer clays (Delvaux *et al.*, 1990a, 1990b).

These clays thus depict a weathering sequence illustrated as follows:

Tropept	→	Udalf	→	Udult
H/Sm with high charge smectite (31% Sm)		H/Sm with high charge smectite (27% Sm) kaolinite		kaolinite H/Sm with lower charge smectite (21% Sm)
H/(H + K) = 0.82		H/(H + K) = 0.63		H/(H + K) = 0.38.

Dispersion was achieved without any chemical pretreatment by the Na^+/resin method (Rouiller *et al.*, 1972; Bartoli *et al.*, 1991). Four clay subfractions of respective nominal size <0.1, 0.1–0.2, 0.2–0.5, and 0.5–2 μm were obtained after continuous flow ultracentrifugation of the whole clay fraction. Their contents were determined after pipetting. Clay subfractions were then deferrated with dark oxalate-oxalic acid pH 3 buffer solution (Blakemore, 1981) and dithionite-citrate-bicarbonate (DCB) (Mehra and Jackson, 1960).

Table 1 gives the respective contents of the clay subfractions as well as their CEC, H/(H + K) ratio, and K^+ affinity.

Two main features appear from the table: (1) The clays extracted from the three pedons are dominated by fine particle size classes; fine clays (<0.2 μm) indeed represent between 68 and 75% of the total clay contents (<2 μm). (2) For each pedon, there is a clear relationship between the clay particle size, CEC, relative halloysite content, and K^+ affinity: the fine clays (<0.2 μm) exhibit the highest CEC, H/(H + K) ratio and K^+ exchange selectivity.

The materials examined in this study consist of the deferrated fine clays of particle size class <0.1 μm and 0.1–0.2 μm, respectively.

X-ray diffraction and FTIR spectroscopy

XRD patterns and IR spectra were obtained by the methodologies described in Delvaux *et al.* (1990b).

TEM

The fine clays (<0.1 and 0.1–0.2 μm) were saturated with K^+ or Mg^{2+}. Respective clay pastes were then homogenized by mechanical stirring and placed in the filtration cells (Tessier and Berrier, 1979) for equilibration with water at a suction pressure of 3.2 kPa (0.032 bar) for 4 days at 20°C. After equilibration, interstitial water was replaced successively by methanol, propylene oxide, and finally Spurr resin. After the resin had hardened, thin sections about 400 Å thick were cut with a diamond knife on a Richert-Jung Ultracut E microtome. TEM observations (120 kV) were carried out using a Philips STEM 420 microscope.

Focusing and photography were accomplished on adjacent areas, so that all images were recorded from areas exposed to the electron beam for the same length of time. The average number of particles per unit area was computed after numbering the particles in an area of 3.95 μm^2 on 18 micrographs.

Table 1. Characteristics of the clay fractions: content of each particle size class relative to total clay; CEC; relative halloysite content with respect to kaolinite; and K^+ exchange selectivity ($K_{G,\ 0.05}$).

Pedon	Clay particle size μm	Weight percent of total clay fraction %	CEC pH 7[1] meq/100 g	H/(H + K)[2]	$K_{G,\ 0.05}$[3] $(mole/L)^{-1/3}$
SN5	<0.1	46.4	32.2	1.0	56.2
	0.1–0.2	25.5	32.1	0.89	63.0
	0.2–0.5	10.4	25.4	0.80	39.5
	0.5–2	13.9	23.2	0.73	32.4
SN2	<0.1	34.3	26.4	0.79	39.6
	0.1–0.2	32.9	24.5	0.69	34.4
	0.2–0.5	14.9	18.3	0.37	22.2
	0.5–2	15.9	14.7	0.25	20.9
MK1	<0.1	50.5	25.0	0.38	14.8
	0.1–0.2	24.1	23.0	0.29	11.2
	0.2–0.5	12.0	17.1	0.21	7.6
	0.5–2	11.7	13.5	0.19	6.4

[1] CEC measured at pH 7 by M ammonium acetate (Mackenzie, 1952).

[2] Relative halloysite content estimated from the XRD intensity ratio $I_{10}/(I_{10} + I_7)$ (Churchman *et al.*, 1984).

[3] Gapon's coefficient (K_G) for equilibrium solutions with 5% K (equivalent fraction) at pH 4 (Delvaux *et al.*, 1988).

Terminology

For a comprehensive characterization of clay minerals, it is necessary to describe clays not only at the scale of the interlayer spacing, but also at higher levels of their structural organization. *Clay texture* refers to particle size (Tessier and Pedro, 1987). The term *clay microstructure* is used for describing both particle size and spatial arrangement involving interparticle void space (Tessier, 1990). *Microstructure* thus involves both intraparticle and interparticle organization of the clay-water system. *Particle frequency* accounts for the number of particles per unit area.

RESULTS AND DISCUSSION

XRD and FTIR characterization

XRD patterns and FTIR spectra are illustrated in Figures 1 and 2, respectively.

XRD data confirm that these fine clays are dominated by 1:1 layer silicates with a decrease in relative halloysite content with respect to kaolinite and increasing weathering (stage SN5 → SN2 → MK1).

The presence of 2:1 swelling clays in halloysite-smectite mixed-layer clays (H/Sm) can be detected in the XRD patterns in the following ways (Delvaux *et al.*, 1990b). (1) The ethylene-glycol saturation of the clays

https://doi.org/10.1346/CCMN.1992.0400409 Published online by Cambridge University Press

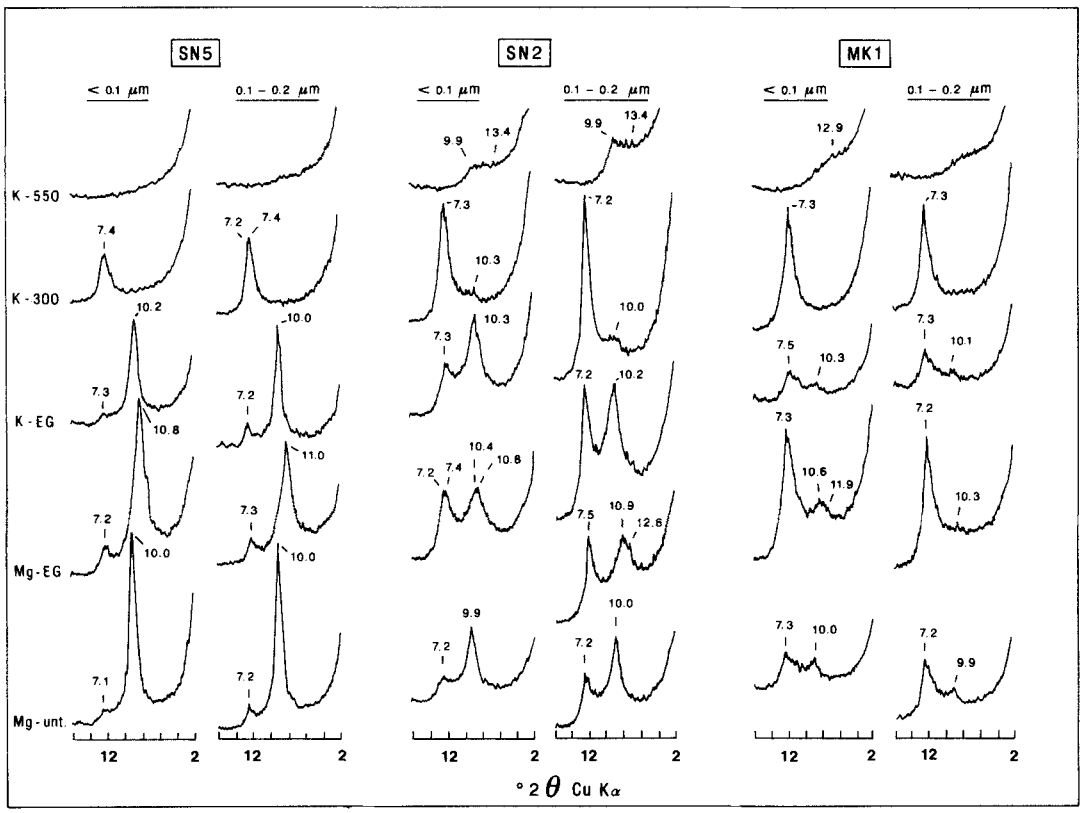

Figure 1. X-ray (CuKα) diffraction patterns of oriented clays SN5, SN2, MK1 of particle size class <0.1 μm and 0.1–0.2 μm after various treatments. Mg-Unt. = Mg^{2+} clay, untreated; Mg-EG = Mg^{2+} clay, ethylene glycol; K-EG = K^+ clay, ethylene glycol; K-300 = K^+ clay, 300°C; K-550 = K^+ clay, 550°C. Spacings in Å.

induces a differential swelling of the reflection close to 10 Å, which depends on the nature of exchangeable cation ($d_{Mg^{2+}-EG} > d_{K^+-EG}$). (2) The thermal treatment at 300°C produces a 7 Å reflection, which is larger than expected for pure anhydrous dioctahedral 1:1 clays, and/or a tailing of that reflection towards the low angle region. Diffraction bands can also be observed around 10 Å. (3) Broad diffraction bands persist in the 10–13 Å region after dehydroxylation of the 1:1 clays (550°C: SN2, MK1).

The FTIR spectra (Figure 2) also show that these clays are dominated by kaolin minerals either rich in halloysite or in kaolinite.

IR spectra performed for fine clays SN5 show all the bands characterizing halloysite (Farmer, 1964; Anton and Rouxhet, 1977). Distinct IR features point to the presence of kaolinite in the clays SN2 and MK1.

The results obtained from XR diffraction and IR spectroscopy clearly complement each other, as illustrated in Table 2. The appearance of the 3652 cm^{-1} IR absorption band as well as the decrease of the absorbance ratio A3700/A3620 (Parker, 1969; Nagasawa and Miyazaki, 1976) are both in good agreement with the decrease of relative halloysite content [H/(H + K)] *vs* A3700/A3620 (r = −0.991), i.e., with increasing kaolinite content and soil weathering stages.

Transmission Electron Microscopy

TEM micrographs are illustrated in Figures 3–7 at various magnifications for very fine (<0.1 μm) or fine

Table 2. Comparison between relative halloysite content with respect to kaolinite [H/(H + K)], IR absorbance ratio A3700/A3620[1] and the absence (−) or presence (+) of a discrete IR absorption at 3650 cm^{-1}.

	Sample					
	SN5		SN2		MK1	
Particle size class (μm)	<0.1	0.1–0.2	<0.1	0.1–0.2	<0.1	0.1–0.2
H/(H + K)	1.00	0.89	0.79	0.69	0.38	0.29
A3700/A3620[1]	0.94	0.98	1.01	1.07	1.30	1.35
3650 cm^{-1}	−	−	+	+	+	+

[1] Ratio (absorbance of the 3700 cm^{-1} band)/(absorbance of the 3620 cm^{-1} band).

https://doi.org/10.1346/CCMN.1992.0400409 Published online by Cambridge University Press

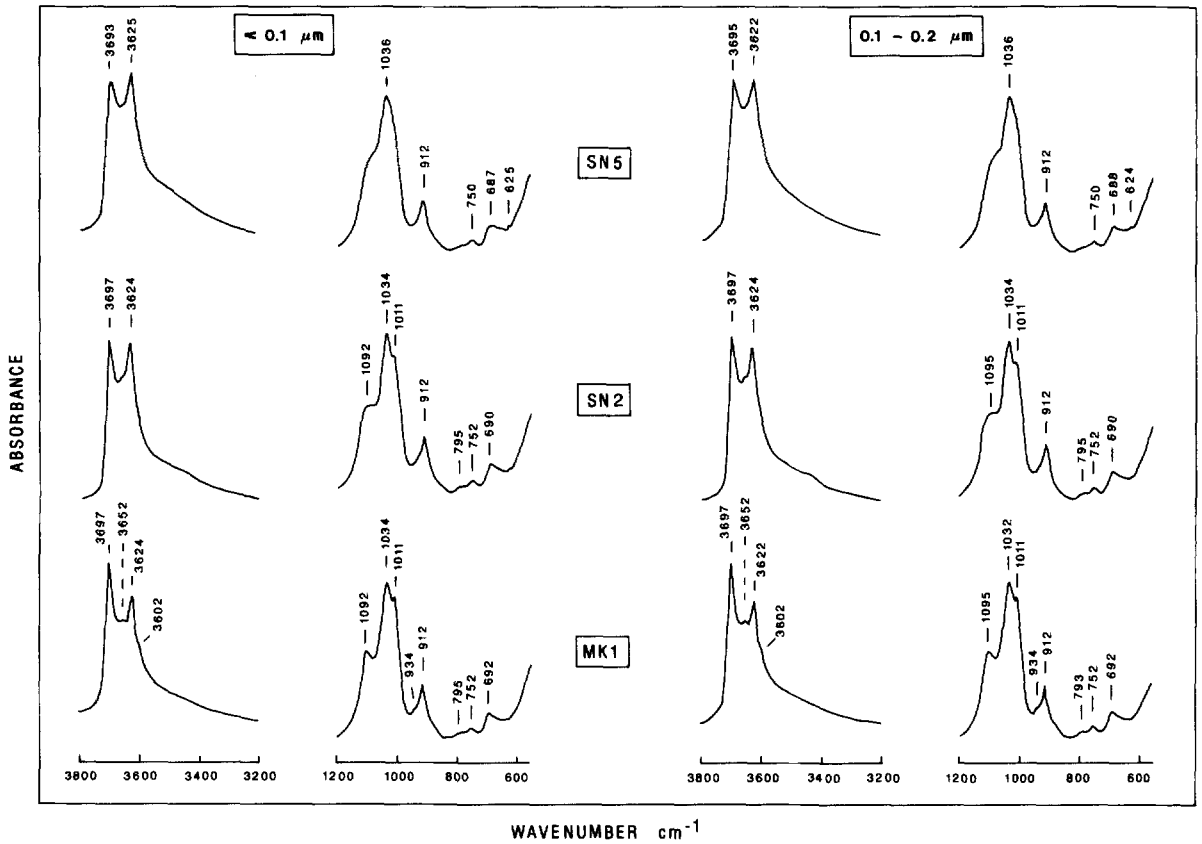

Figure 2. FTIR spectra of dehydrated clays SN5, SN2, MK1 of particle size <0.1 μm (left) and 0.1–0.2 μm (right).

(0.1–0.2 μm) clays saturated with K^+ or Mg^{2+} and hydrated under a low suction pressure (P = 3.2 kPa).

Methodological considerations. Figure 3 illustrates the microstructure of the hydrated Mg^{2+} clay SN5 <0.1 μm. Thin sections recorded at low magnification show a very homogeneous distribution of particles at this scale. A similar homogeneity was observed for all samples.

Comparison of Figures 4 and 5 obtained for <0.1 and 0.1–0.2 μm Mg^{2+} clays, respectively, illustrates the efficiency of the dispersion with Na^+ resin prior to continuous flow ultracentrifugation. Whatever the shape of the particles, their size is indeed distinctly larger in the fraction 0.1–0.2 μm (Figure 5).

An important observation from Figure 4a (see h labels) is that there is no evidence of dehydration stress for halloysite spheroids, revealed by gaps between books of crystal layers with a typical "core and crust" appearance (Kirkman, 1977; Kohyama *et al.*, 1978, 1982; Saigusa *et al.*, 1978).

Lack of dehydration stress, also supported by Figures 5a and 6a (see h labels), suggests that replacement of water by the solvents used before preparing the ultrathin sections does not disturb the general arrangement of the hydrated particles (Tessier, 1984; Ben Rhaïem *et al.*, 1987).

Particle shape and weathering stage. Important variations occurring with increasing soil weathering (SN5 → SN2 → MK1; Figures 4a, 4b, and 4c, respectively) can be seen by the morphology of the clay particles. The dominant particle shape in SN5 (a) is spheroidal (S), but a few particles have a tubular shape. The most frequent morphology in SN2 (b) is tubular (T). In MK1 (c), the particles have a planar shape (P). The dominant particle morphologies are thus associated here with the three soil weathering stages: spheroids (SN5), tubes

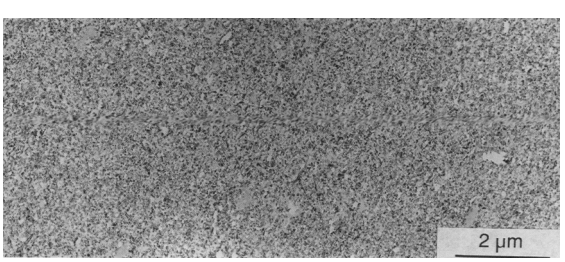

Figure 3. TEM micrograph of clay SN5 <0.1 μm, previously saturated with Mg^{2+} and hydrated (P = 3.2 kPa).

https://doi.org/10.1346/CCMN.1992.0400409 Published online by Cambridge University Press

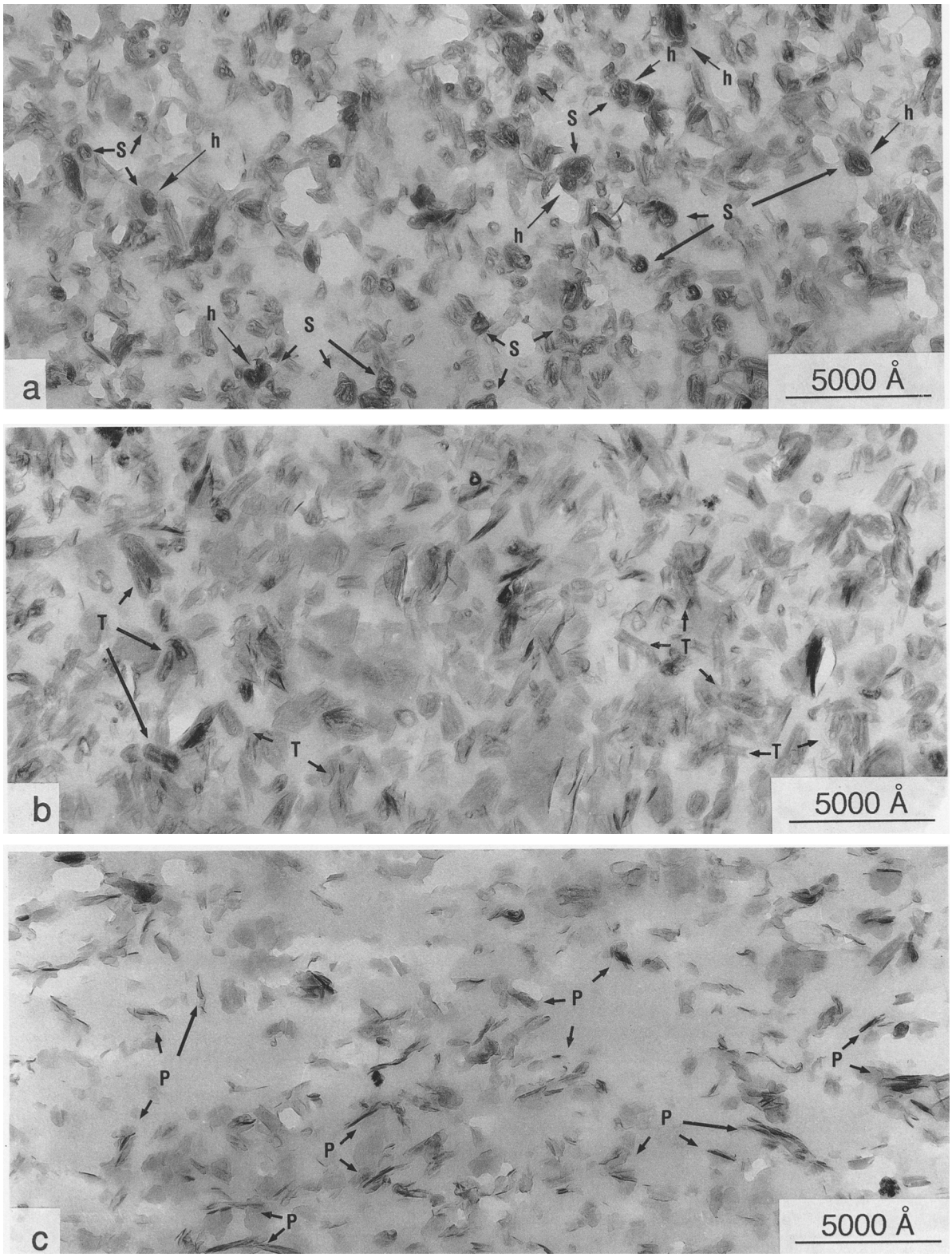

Figure 4. TEM micrographs of Mg^{2+} saturated clays <0.1 μm prepared at 3.2 kPa suction pressure. (a) SN5; (b) SN2; (c) MK1. Lack of dehydration stress is labeled by h arrows. Spheroidal, tubular, and platy shapes are labeled by S, T, and P arrows, respectively.

https://doi.org/10.1346/CCMN.1992.0400409 Published online by Cambridge University Press

Table 3. Average number of particles per μm^2 as influenced by exchangeable cation for the particle size class 0.1–0.2 μm (average values computed from 18 micrographs of 3.95 μm^2 area).

Exchangeable cation	Average number of particles per μm^2		
	SN5	SN2	MK1
Mg^{2+}	63.52 ± 6.08	50.94 ± 5.95	31.66 ± 4.09
K^+	44.82 ± 3.05	35.83 ± 2.66	27.86 ± 3.07

(SN2), and platelets (MK1). Similar trends in morphological features appear from Figures 5 and 6 where subscripts a, b, and c also refer to SN5, SN2, and MK1, respectively. Spheroidal and tubular shapes are characteristic of halloysite while planar morphologies are more typical of kaolinite (Dixon, 1989). Such variations in particle shape are in good agreement with XRD and IR data. In tropical soils from other volcanic areas, similar variations in morphology are also related to the weathering stage: spheroids dominate in recent halloysitic soils, tubes predominate in more weathered soils and, at a more advanced stage of weathering, kaolinite (platelets) is the dominant clay mineral (Quantin, 1991).

Literature data generally indicate that various halloysite shapes may coexist in the same clay fraction (Tazaki, 1982). They suggest that halloysite morphologies may vary according to the type of "precursor": Spheroids would form from allophane and volcanic glass (Nagasawa and Miyazaki, 1976; Kirkman, 1981) and tubes from feldspars (Parham, 1969). Our results support the view that the shapes of pedogenic halloysite can also be related to the soil weathering stage, confirming the observations carried out by Quantin (1990 and 1991).

Particle frequency and weathering stage. Variations in particle frequency, i.e., the amount of particles per unit area, are also related to the soil weathering stage. Particle frequency (Figure 4) sharply decreases when soil weathering increases, with the highest number of particles per unit area in SN5 (a) and the lowest in MK1 (c). A similar decrease in particle frequency is also observed for the clays 0.1–0.2 μm in Figures 5 and 6, and is supported by Table 3. The decrease in particle frequency from increasing soil weathering can be related to a decrease in the layer charge of the clay minerals from SN5 to MK1, as inferred from Table 1. In strongly hydrated systems made of pure homoionic 2:1 swelling clays, it is established that the number of particles per unit area decreases with decreasing layer charge (Tessier, 1984; Tessier and Pedro, 1987; Touret *et al.*, 1990).

Microstructure and the nature of exchangeable cation. Figures 5 and 6 present TEM micrographs obtained for fine clays 0.1–0.2 μm saturated with Mg^{2+} and K^+ respectively. Related values of the average number of particles per unit area are shown in Table 3.

They point out two main features. (1) For each clay of distinct origin (a, b, c, i.e., SN5, SN2, MK1), both the number of particles per unit area and particle size decrease distinctly after K^+ saturation. The decrease in particle size after K^+ saturation is particularly visible for clay SN5 (Figures 5a and 6a), with an average particle size of about 800 Å and 600 Å after Mg^{2+} and K^+ saturation. (2) The decrease in particle frequency and particle size induced by the exchangeable cation (Table 3) become less pronounced as soil weathering increases [SN5 (a) → MK1 (c)], i.e., CEC decreases (Table 1).

The exchangeable cation has a marked effect on clay particle aggregation (size and frequency of occurrence). Aggregation involves regrouping of initial K^+ particles, which not only affects particle size but also the number of particles per unit area, i.e., the spatial arrangement. Marked aggregation due to Mg^{2+} saturation is observed at both intraparticle and interparticle levels, particularly for clay SN5.

After Mg^{2+} saturation (Figure 5a), the particles themselves indeed show a larger average size and the average interparticle size is lower compared to K^+ saturation (Figure 6a). These observations suggest a higher average number of layers per particle and a lower water content for the Mg^{2+} saturated clays than for the K^+ saturated clays.

The replacement of K^+ by Mg^{2+} on the exchange sites induces an increase in cohesion forces at intraparticle and interparticle levels. This variation in the organization as a function of the nature of exchangeable cation is similar to that of smectites (Tessier, 1984). For the clays studied, exchangeable K^+ thus behaves at high water content as a dispersing ion. This occurs also for hydrated K^+ and Na^+ low charge smectites (Tessier, 1987).

At high water content (P = 3.2 kPa), the texture and microstructure of these kaolin rich clays thus depend markedly on the nature of the exchangeable cation and the layer charge of the clay minerals. Such a behavior is not typical for either pure 1:1 clays or high charge illites, but is well-known for 2:1 low charge swelling clays (≃0.4 charge unit per half cell) (Tessier, 1984; Ben Rhaïem *et al.*, 1987; Tessier and Pedro, 1987). Furthermore, for a given cation, particle size and water content (i.e., interparticle void space) increase and decrease, respectively, as the layer charge of the 2:1 swelling clays increases (Tessier, 1984; Tessier and Pedro, 1987; Touret *et al.*, 1990). The TEM observations presented here therefore suggest a decrease in layer charge of the clay minerals which is effectively in agreement with the CEC values and K^+ selectivity coefficients given in Table 1.

These relationships are in good agreement with the results obtained for the whole clay fractions (<2 μm) extracted from the same soils: the presence of smectite

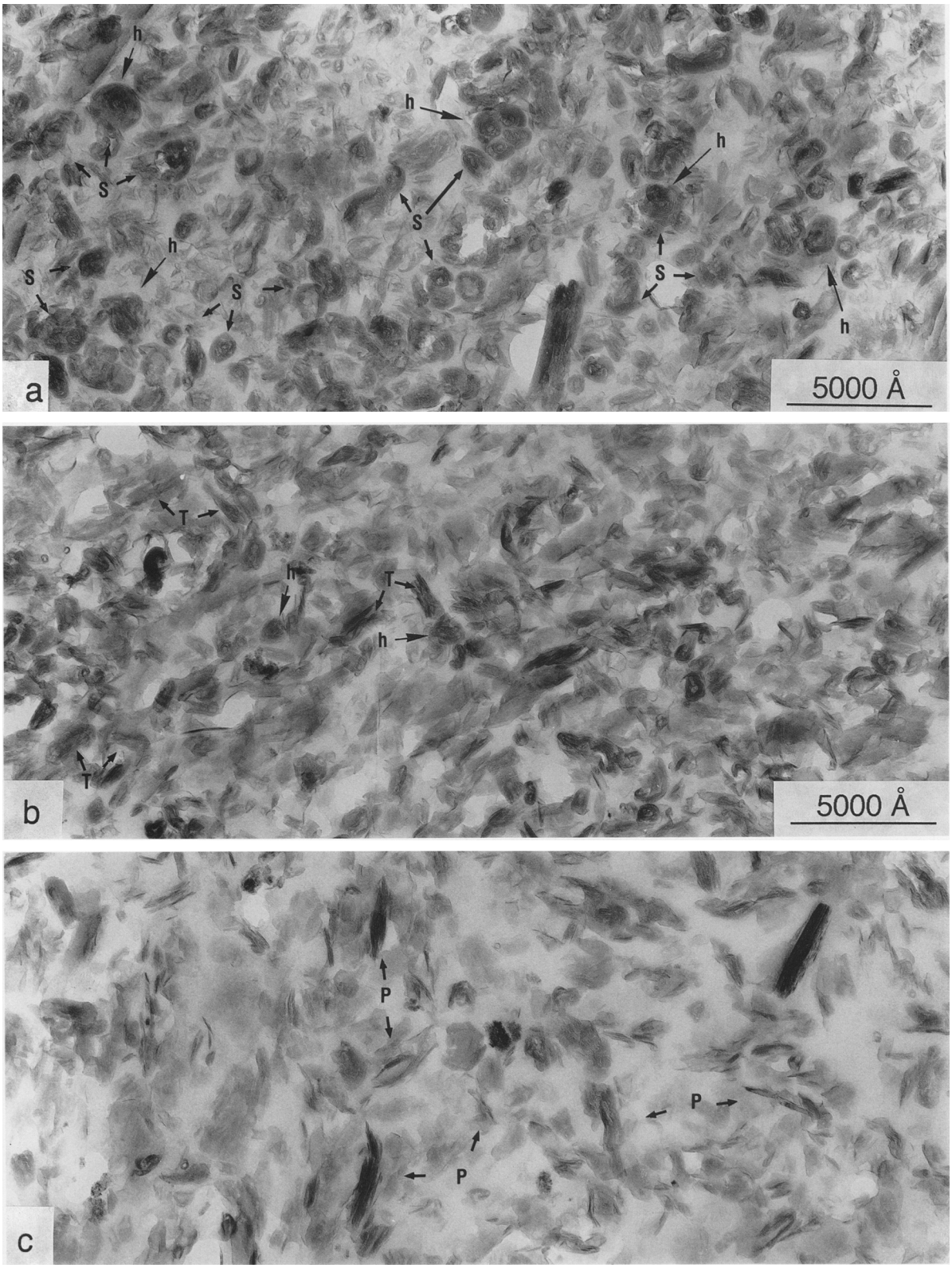

Figure 5. TEM micrographs of Mg^{2+} saturated clays 0.1–0.2 μm prepared at 3.2 kPa suction pressure. (a) SN5; (b) SN2; (c) MK1. (h, S, T, P: see legend of Figure 4).

https://doi.org/10.1346/CCMN.1992.0400409 Published online by Cambridge University Press

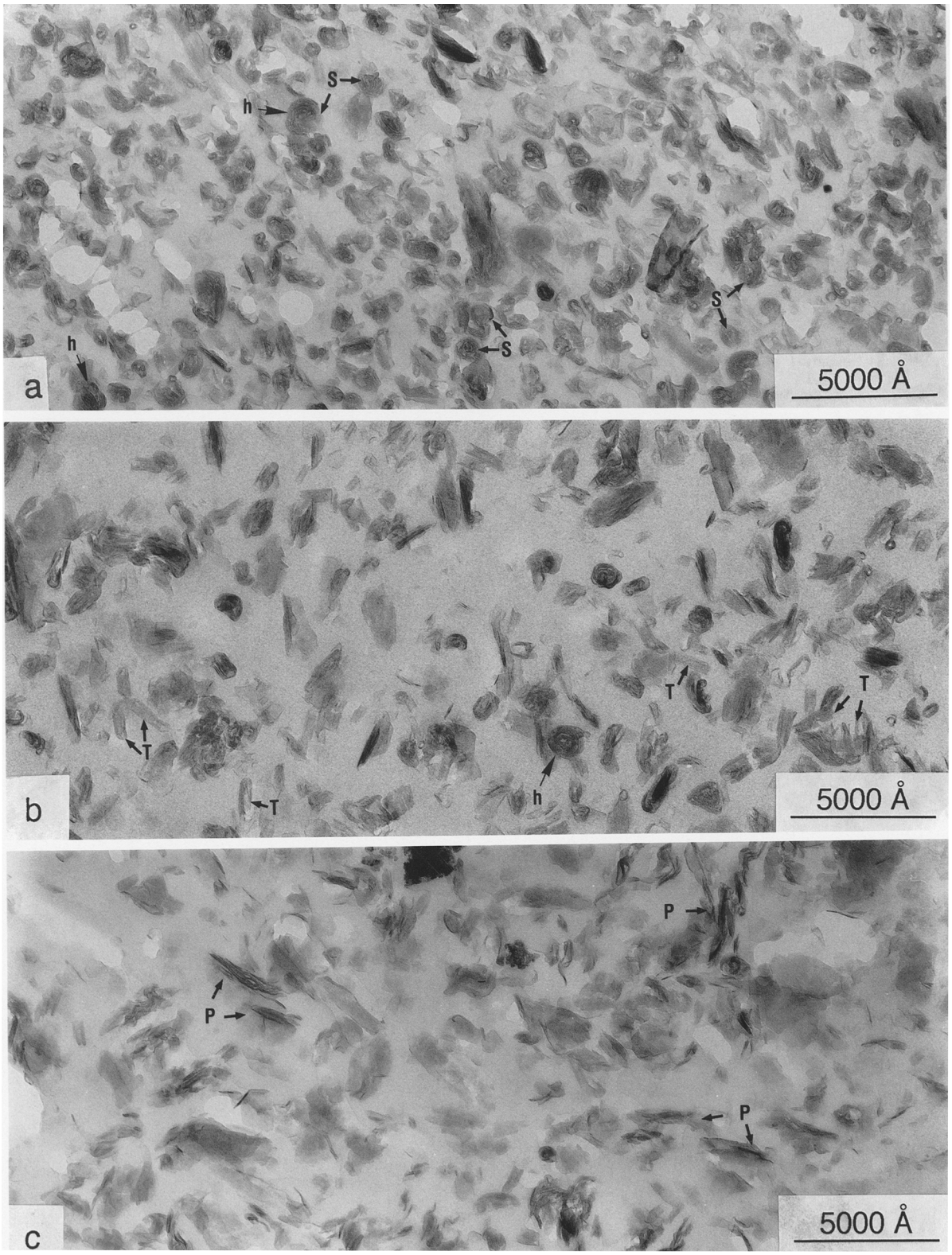

Figure 6. TEM micrographs of K^+ saturated clays 0.1–0.2 μm prepared at 3.2 kPa suction pressure. (a) SN5; (b) SN2; (c) MK1. (h, S, T, P: see legend of Figure 4).

https://doi.org/10.1346/CCMN.1992.0400409 Published online by Cambridge University Press

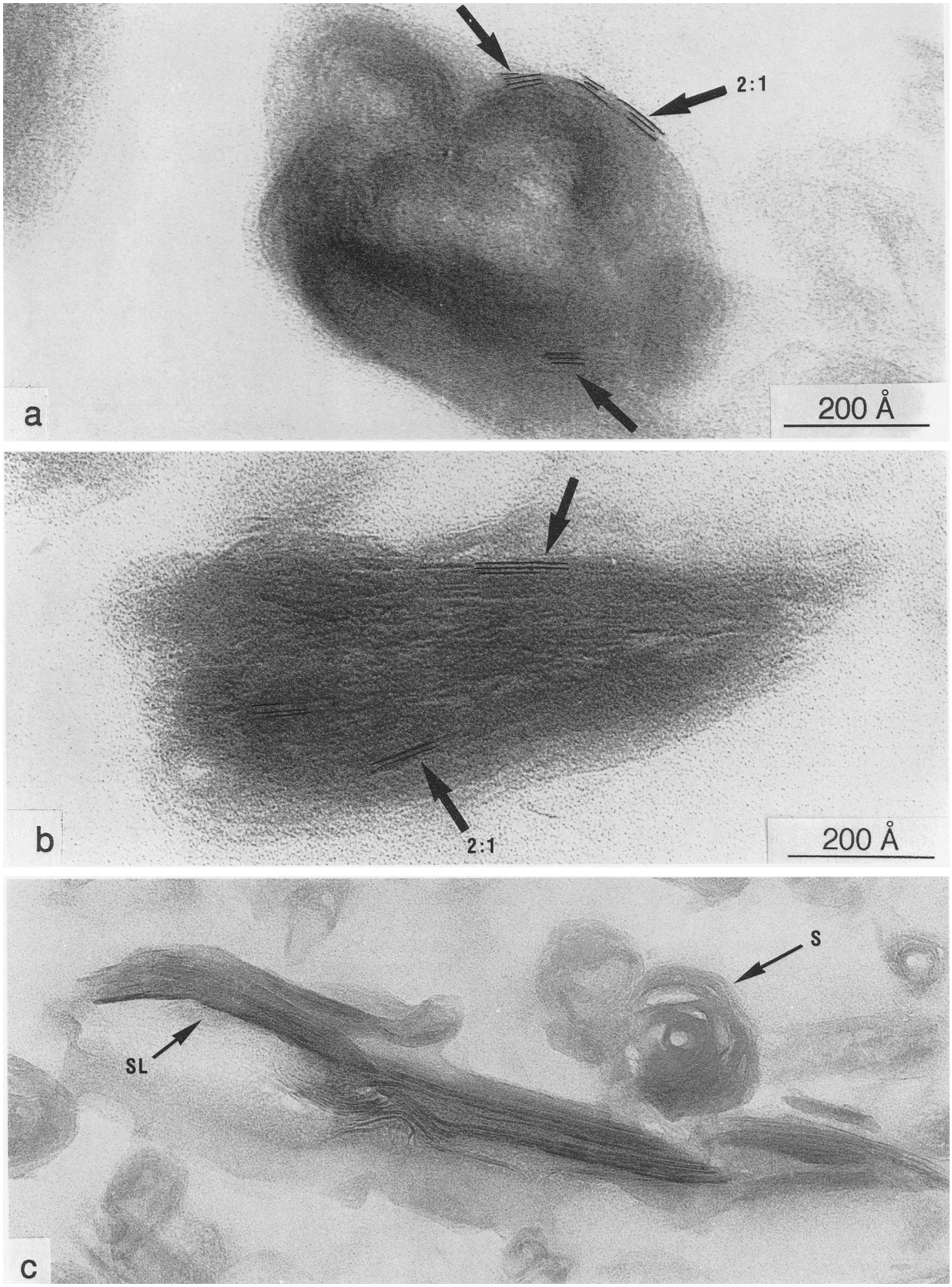

Figure 7. TEM observations of K^+ saturated clay SN5 0.1–0.2 μm (3.2 kPa). (a, b) 2:1 layers are labeled; (c) spheroidal (S) and sheet-like (SL).

https://doi.org/10.1346/CCMN.1992.0400409 Published online by Cambridge University Press

in H/Sm mixed-layer clays, and the decrease in smectite layer charge, relative halloysite content, CEC and K^+ affinity, with increasing soil weathering stage (Delvaux *et al.*, 1990b).

Identification of 2:1 layers. The presence of 2:1 layers in these materials is illustrated for K^+ clay SN5 (0.1–0.2 μm) in Figures 7a and 7b. These micrographs show that 2:1 layers are present in the quasi spheroidal shape of halloysite, as previously observed (Quantin *et al.*, 1988). The 2:1 layers mostly appear at the periphery of the particles. Such a localization may explain (1) the distinct variations in texture and microstructure of these clays, as influenced by the nature of the exchangeable cation, and (2) the important effect of small amounts of smectite on the behavior of these kaolin rich clays.

In the same K^+ clay SN5 (0.1–0.2 μm), some particles exhibit a sheet-like appearance: This shape (SL label) can be seen in Figure 7c together with a typical halloysite spheroid (S label). As far as the sheet-like particle is concerned, the lateral extension of the layers is wide (≃1400 Å) and the thickness reaches about 110 Å. This sheet-like organization is similar to that of low charge smectites (Ben Rhaïem *et al.*, 1987).

Figure 7c further suggests that the central part of the sheet-like particle consists of a "remnant" spheroid. In halloysite, the dissymmetry of the 1:1 layers and the surface tension, due to the hydrophobic nature of the external surface of uncharged 1:1 layers, are likely to be the main mechanisms for curved and rolled shapes (Bailey, 1990). By contrast, the symmetry of the 2:1 layers, associated with strong interlayer cohesion forces due to exchangeable cations, tends to make flat and large clay particles in hydrated media (Kohyama *et al.*, 1982). Thus, Figure 7c illustrates in sample SN5 that there are a few particles made of enough adjacent 2:1 layers to prevent the development of rolled or curved shapes due to halloysite.

CONCLUSIONS

Results obtained from XRD, FTIR, and TEM converge to show that the clays studied are rich in kaolin minerals. They depict a sequence where kaolinite content progressively increases at the expense of hydrated halloysite with increased soil weathering. Accordingly, particle shape varies in the following way: spheroids → tubes → platelets.

Smectite, in small amounts, is closely associated with halloysite. 2:1 layers are localized in the halloysite habitus, but mostly at the particle periphery.

At high water content, both clay texture and microstructure are influenced by the nature of the exchangeable cation and layer charge of the 2:1 layers. Particle size and number per unit area both decrease after K^+ saturation and the effects of the nature of exchangeable cation become less pronounced with the decreasing layer charge of the 2:1 units, i.e., with increased soil weathering. These important variations in microstructure are related to the localization of the 2:1 layers at the periphery of the clay particles. These variations show that, at high water content, small amounts of smectite have a major effect on the organization of clay systems dominated by kaolin minerals, at both the intraparticle and interparticle levels.

The good agreement between the results presented here and in previous related studies carried out on these clays (Delvaux *et al.*, 1990a and 1990b) has to be pointed out. CEC, K^+ affinity, smectite content, layer charge, and the effect of the nature of exchangeable cation on clay texture and microstructure all decrease with an increase in soil weathering.

Finally, these results are applicable to the conditioning of homoionic clays at water potentials which are realistic with respect to field conditions. Both texture and microstructure can be observed and discussed at equal water energy levels. These advances improve our ability to predict soil properties.

ACKNOWLEDGMENTS

Thanks are due to the editor and the referees for their comments and suggestions. The authors are also indebted to Dr. W. Stone for reviewing the English phraseology.

REFERENCES

Anton, O. and Rouxhet, P. G. (1977) Note on the intercalation of kaolinite, dickite and halloysite by dimenthylsulfoxide: *Clays & Clay Minerals* **25,** 259–263.

Bailey, S. W. (1990) Halloysite—A critical assessment: in *Proc. 9th Int. Clay Conf. Strasbourg, 1989,* V. C. Farmer and Y. Tardy, eds., Sci. Géol. Mém. **86,** 89–98.

Bartoli, F., Burtin, G., and Herbillon, A. J. (1991) Disaggregation and clay dispersion of oxisols: Na resin, a recommended methodology: *Geoderma* **49,** 307–377.

Ben Rhaïem, H., Pons, C. H., and Tessier, D. (1987) Factors affecting the microstructure of smectites: Role of cation and history of applied stress: *Proc. 8th Int. Clay Conf. Denver, 1985,* L. G. Schultz, H. van Olphen, and F. A. Mumpton, eds., The Clay Minerals Society, Bloomington, Indiana, 292–297.

Blakemore, L. C. (1981) Acid oxalate extractable iron, aluminum, and silicon: *Circular letter n°5,* appendix 1, ICOMAND, New Zealand Soil Bureau, Lower Hutt, New Zealand.

Churchman, G. I., Whitton, J. S., Claridge, G. C. C., and Theng, B. K. G. (1984) Intercalation method for differentiating halloysite from kaolinite: *Clays & Clay Minerals* **32,** 241–248.

Delvaux, B., Herbillon, A. J., and Vielvoye, L. (1989) Characterization of a weathering sequence of soils derived from volcanic ash in Cameroon. Taxonomic, mineralogical and agronomic implications: *Geoderma* **45,** 375–388.

Delvaux, B., Herbillon, A. J., Dufey, J. E., and Vielvoye, L. (1990a) Surface properties and clay mineralogy of hydrated halloysitic soil clays. I: Existence of interlayer K^+ specific sites: *Clay Miner.* **24,** 617–630.

Delvaux, B., Herbillon, A. J., Vielvoye, L., and Mestdagh, M. M. (1990b) Surface properties and clay mineralogy of hydrated halloysitic soil clays. II: Evidence for the presence

of halloysite/smectite (H/Sm) mixed-layer clays: *Clay Miner.* **25,** 141–160.

Delvaux, B., Herbillon, A. J., Dufey, J. E., Burtin, G., and Vielvoye, L. (1988) Adsorption sélective du potassium par certaines halloysites (10 Å) de sols tropicaux développés sur roches volcaniques. Signification minéralogique: *C.R. Acad. Sci. Paris,* **T. 307, série II,** 311–317.

Dixon, J. B. (1989) Kaolin and serpentine group minerals: in *Minerals in Soil Environments,* J. B. Dixon and S. B. Weed, eds., Soil Science Society of America Book Series n°1, 467–526.

Farmer, V. C. (1964) *The Infrared Spectra of Minerals*: Mineralogical Society, London.

Kirkman, J. H. (1977) Possible structure of halloysite disks and cylinders observed in some New Zealand rhyolitic tephras: *Clay Miner.* **12,** 199–216.

Kirkman, J. H. (1981) Morphology and structure of halloysite in New Zealand tephras: *Clays & Clay Minerals* **29,** 1–9.

Kohyama, N., Fukushima, K., and Fukami, A. (1978) Observation of the hydrated form of tubular halloysite by an electron microscope equipped with an environmental cell: *Clays & Clay Minerals* **26,** 25–40.

Kohyama, N., Fukushima, K., and Fukami, A. (1982) Interlayer hydrates and complexes of clay minerals observed by electron microscopy using an environmental cell: in *Proc. 7th Int. Clay Conf. Bologna and Pavia, 1981,* H. van Olphen and F. Veniale, eds., Elsevier, Amsterdam, 373–384.

Mackenzie, R. C. (1952) A micromethod for determination of cation exchange capacity of clays: *Clay Miner. Bull.* **1,** 203–205.

Mehra, O. P. and Jackson, M. L. (1960) Iron oxides removal from soils and clays by dithionite-citrate system buffered with sodium bicarbonate: *Clays & Clay Minerals* **5,** 317–327.

Nagasawa, K. and Miyazaki, S. (1976) Mineralogical properties of halloysite as related to its genesis: in *Proc. 6th Int. Conf. Mexico City, 1975,* S. W. Bailey, ed., Wilmette, Illinois, 256–265.

Parham, W. E. (1969) Formation of halloysite from feldspar: Low temperature, artificial weathering versus natural weathering: *Clays & Clay Minerals* **17,** 13–22.

Parker, T. W. (1969) A classification of kaolinites by infrared spectroscopy: *Clay Miner.* **8,** 135–141.

Quantin, P. (1990) Specficity of the halloysite-rich tropical or subtropical soils: *Transactions 14th International Congress of Soil Science, Kyoto, 1990,* **vol. VII,** International Society of Soil Science, 16–21.

Quantin, P. (1991) Les sols de l'archipel volcanique des Nouvelles-Hébrides (Vanuatu). Etude de la pédogenèse initiale en milieu tropical: Thèse, U.E.R. des Sciences de la Vie et de la Terre, Institut de Géologie, Strasbourg.

Quantin, P., Gautheyrou, J., and Lorenzoni, P. (1988) Halloysite formation through *in situ* weathering of volcanic glass from trachytic pumices, Vico's Volcano, Italy: *Clay Miner.* **23,** 423–437.

Rouiller, J., Burtin, G., and Souchier, B. (1972) La dispersion des sols dans l'analyse granulométrique. Méthode utilisant les résines échangeuses d'ions: *Bulletin ENSAIA Nancy* **XIV,** 193–205.

Saigusa, M., Shoji, S., and Kato, T. (1978) Origin and nature of halloysite in Ando soils from Towada tephra, Japan: *Geoderma* **20,** 115–129.

Tazaki, K. (1982) Analytical electron microscopic studies of halloysite formation processes. Morphology and composition of halloysite: in *Proc. 7th Int. Clay Conf., Bologna and Pavia, 1981,* H. van Olphen and F. Veniale, eds., Developments in Sedimentology **27,** 573–584.

Tessier, D. (1984) Etude expérimentale de l'organisation des matériaux argileux: Hydratation, gonflement et structuration au cours de la dessication et de la réhumectation: Thèse Univ. Paris VII, INRA Versailles.

Tessier, D. (1987) Identification of clays. Data from investigations with strongly hydrated systems: in *Methodology in Soil-K Research, Proc. 20th Colloquium Int. Potash Institute,* International Potash Institute, Bern, Switzerland, 45–63.

Tessier, D. (1990) Behaviour and microstructure of clay minerals: in *Soil Colloids and Their Associations in Aggregates, Ghent, 1984,* M. F. De Boodt, M. H. B. Hayes, and A. J. Herbillon, eds., NATO ASI, Series B: *Physics* **215,** 387–415.

Tessier, D. and Berrier, J. (1979) Utilisation de la microscopie électronique à balayage dans l'étude des sols. Observation de sols humides soumis à différents pF: *Science du Sol* **1,** 67–82.

Tessier, D. and Pedro, G. (1987) Mineralogical characterization of 2:1 clays in soils: Importance of the clay texture: in *Proc. 8th Int. Clay Conf., Denver, 1985,* L. G. Schultz, H. van Olphen, and F. A. Mumpton, eds., The Clay Minerals Society, Bloomington, Indiana, 78–84.

Touret, O., Pons, C. H., Tessier, D., and Tardy, Y. (1990) Etude de la répartition de l'eau dans des argiles saturées Mg^{2+} aux fortes teneurs en eau: *Clay Miner.* **25,** 217–233.

(Received 25 November 1991; accepted 14 July 1992; Ms. 2159)